Guidelines for processing RBR CTD profiles

Mark Halverson, Jen Jackson, Clark Richards, Humfrey Melling, Brian Hunt, Ray Brunsting, Mike Dempsey, Germaine Gatien, Andrew Hamilton, Wayne Jacob, Sarah Zimmerman

Fisheries and Oceans Canada
Institute of Ocean Science
9860 West Saanich Road
Sidney, British Columbia
V8L 4B2

2017

Canadian Technical Report of Hydrography and Ocean Sciences 314

Fisheries and Oceans Canada
Pêches et Océans Canada
Canada

Canadian Technical Report of Hydrography and Ocean Sciences

Technical reports contain scientific and technical information of a type that represents a contribution to existing knowledge but which is not normally found in the primary literature. The subject matter is generally related to programs and interests of the Oceans and Science sectors of Fisheries and Oceans Canada.

Technical reports may be cited as full publications. The correct citation appears above the abstract of each report. Each report is abstracted in the data base *Aquatic Sciences and Fisheries Abstracts*.

Technical reports are produced regionally but are numbered nationally. Requests for individual reports will be filled by the issuing establishment listed on the front cover and title page.

Regional and headquarters establishments of Ocean Science and Surveys ceased publication of their various report series as of December 1981. A complete listing of these publications and the last number issued under each title are published in the *Canadian Journal of Fisheries and Aquatic Sciences*, Volume 38: Index to Publications 1981. The current series began with Report Number 1 in January 1982.

Rapport technique canadien sur l'hydrographie et les sciences océaniques

Les rapports techniques contiennent des renseignements scientifiques et techniques qui constituent une contribution aux connaissances actuelles mais que l'on ne trouve pas normalement dans les revues scientifiques. Le sujet est généralement rattaché aux programmes et intérêts des secteurs des Océans et des Sciences de Pêches et Océans Canada.

Les rapports techniques peuvent être cités comme des publications à part entière. Le titre exact figure au-dessus du résumé de chaque rapport. Les rapports techniques sont résumés dans la base de données *Résumés des sciences aquatiques et halieutiques*.

Les rapports techniques sont produits à l'échelon régional, mais numérotés à l'échelon national. Les demandes de rapports seront satisfaites par l'établissement auteur dont le nom figure sur la couverture et la page de titre.

Les établissements de l'ancien secteur des Sciences et Levés océaniques dans les régions et à l'administration centrale ont cessé de publier leurs diverses séries de rapports en décembre 1981. Vous trouverez dans l'index des publications du volume 38 du *Journal canadien des sciences halieutiques et aquatiques*, la liste de ces publications ainsi que le dernier numéro paru dans chaque catégorie. La nouvelle série a commencé avec la publication du rapport numéro 1 en janvier 1982.

Canadian Technical Report of Hydrography and Ocean Sciences 314

2017

Guidelines for processing RBR CTD profiles

by

Mark Halverson[123], Jen Jackson[2], Clark Richards[34], Humfrey Melling[5], Brian Hunt[12], Ray Brunsting[2], Mike Dempsey[5], Germaine Gatien[5], Andrew Hamilton[1], Wayne Jacob[2], Sarah Zimmerman[5]

Fisheries and Oceans Canada
Institute of Ocean Science
9860 West Saanich Road
Sidney, British Columbia
V8L 4B2

[1]Department of Earth, Ocean, and Atmospheric Sciences, University of British Columbia, Vancouver, BC, Canada, V6T 1Z4
[2]Hakai Institute, Heriot Bay, BC, Canada
[3]RBR Ltd., Ottawa, ON, Canada
[4]Fisheries and Oceans Canada, Dartmouth, NS, Canada
[5]Fisheries and Oceans Canada, Sidney, BC, Canada

Cat. No. Fs97-18/314E-PDF ISBN 978-0-660-06003-3 ISSN 1488-5417

Correct citation for this publication:

Halverson, M., Jackson, J., Richards, C., Melling, H., Brunsting, R., Dempsey, M., Gatien, G., Hamilton, A., Hunt, B., Jacob, W., and Zimmerman, S. 2017. Guidelines for processing RBR CTD profiles. Can. Tech. Rep. Hydrogr. Ocean Sci. 314: iv + 38 p.

Contents

Abstract

A series of post-processing steps have been developed to improve data quality from RBR loggers when used for vertical profiling. At present, RBR does not provide any official guidance or software for this purpose even though untreated profile data exhibit some classic problems such as salinity spiking. The steps developed and detailed herein apply specifically to the generation of loggers which have a black or gray cylindrical conductivity sensor coil, and a thermistor mounted on the sensor cap. However, some of the processing steps are somewhat generic to any profiler, and are therefore applicable to some degree to the newer generation of RBR instruments that feature a more hydrodynamic conductivity cell and a co-located thermistor.

The post-processing steps include 1) correcting for zero-order holds (optional), 2) data despiking (optional), 3) removing atmospheric pressure, 4) low pass filtering, 5) sensor alignment, 6) descent rate thresholding, 7) derived variables, and 8) bin averaging. Most of the parameters in these steps were found by analyzing field data, as opposed to conducting laboratory tank studies or comparing the data to well-characterized reference sensors. We also provide some basic recommendations for obtaining high quality profiles in the field.

While the primary focus of the processing concerns conductivity, temperature, and pressure, RBR loggers also interface with external sensors (e.g., fluorescence and dissolved oxygen). We will briefly discuss these sensors with special emphasis on the JFE Alec Co. RINKO III O_2 optode.

Résumé

Plusieurs étapes de post-traitement ont été développées afin d'accroître la qualité des profils verticaux issus des CTD produites par RBR. A l'heure actuelle, RBR ne fourni aucune recommandation, ni aucun logiciel permettant de corriger les problèmes classiques que l'on trouve dans les données de profil brut, comme les pics de salinité. Les méthodes développées ici s'appliquent aux modèles possédant un senseur cylindrique noir ou gris, ainsi qu'un thermistor monté sur le cache du senseur. Cependant, certaines étapes du traitement sont génériques, et restent applicables à n'importe quel profiler, ainsi qu'à la nouvelle génération d'instruments produits par RBR, qui utilisent un capteur de conductivité, associé à un thermistor, ayant une meilleure hydrodynamique.

Les étapes de post-traitement incluent 1) la correction des "zero-order holds" (optionnel), 2) la suppression des pics (optionnel), 3) la suppression de la pression atmosphérique, 4) un filtrage par utilisation de filtres passe-bas, 5) l'alignement du senseur, 6) le filtrage des données en fonction d'un seuil de vitesse de descente 7) le calcul des quantités dérivées, et 8) le calcul de la moyenne par cellules. Alors que la plupart des études utilisent des données de laboratoire en réservoir, ou comparent des données de référence capteur, la plupart des paramètres de ces étapes ont ici été validées en analysant des données de terrain.

Bien que le but premier du traitement concerne la conductivité, la température et la pression, les CTD RBR s'interfacent également avec des senseurs externes (e.g., fluorescence et oxygène dissous). Nous discuterons brièvement de ces senseurs, et particulièrement de l'optode JFE Alec Co. Rinko III O2.

1 Introduction

RBR conductivity-temperature-depth (CTD) profilers provide high quality data straight from the instrument without post-processing. However, as we will show, applying additional processing steps, such as carefully aligning the sensors in time, will improve the data and reduce artifacts such as salinity spiking. Unlike Seabird Electronics, RBR does not presently make available any software or guidelines to help with the processing, although their Matlab software, rsktools, will eventually have this functionality. After speaking with staff at RBR, and a number of RBR users in the oceanographic community, it became clear that there are steps which should be taken to ensure high quality data.

Staff scientists at the Hakai Institute, a scientific research institution that conducts long-term research at remote locations on the coastal margin of British Columbia, convened two workshops consisting of experienced RBR and Seabird users to share data processing procedures and to develop a standard post-processing workflow. Application of this workflow to data from a properly calibrated RBR profiler will ensure it is of the highest quality, and therefore suitable for publication in peer-reviewed literature and for distribution to data archives.

1.1 Workshops

The first workshop was help on November 19, 2015 at the Institute of Ocean Sciences in Sidney, British Columbia, Canada. The goal of the workshop was to discuss the processing procedures used by various organizations and researchers. Participants presented their RBR processing strategy and experience with the instruments. The outcome was the formation of working groups, each tasked with a specific objective related to CTD processing (e.g., sensor alignment, filtering, descent rate). Many of the tasks are similar to those used in the Seabird processing chain, and thus we include the Seabird terminology for reference. The working groups were:

- Collection of field data
- Data conversion
- Atmospheric pressure
- Filter
- Align
- Descent rate / “Loop edit”
- Despiking / “Wild edit”
- Ancillary data (e.g., O_2, Turbidity)
- Derived variables

- Technical paper

The second workshop was held on February 1, 2016 at the Institute of Ocean Sciences. The goal of this workshop was to have each working group present its findings. Following the presentations, there was an open discussion to determine the next steps. It was decided that a technical report detailing the steps required to process RBR profiles would be written. The data collection and processing steps suggested in the two workshops and in the different working groups are outlined below.

1.2 Summary of recommended processing steps

Here we summarize the processing steps developed by the RBR working group. The parameters for each step (e.g. conductivity delay) are appropriate for a 6 Hz instrument descending at about 1 m/s with a RINKO III oxygen sensor in a coastal region. The steps are arranged in the recommended order in which they should be applied.

1. [Optional] Zero-order hold correction (Section 5.1)
   (a) Apply to instruments that have zero-order holds
2. [Optional] Data despiking (Section 5.2)
   (a) Identify spikes with median filter and either interpolate over, remove, or replace with `NaN`
3. Correct for atmospheric pressure (Section 5.3)
   (a) Subtract atmospheric pressure from measured total pressure. Estimate atmospheric pressure by:
      i. Using the total pressure measured in air before or after the cast
      ii. For thresholding instruments, use the minimum total pressure at the minimum conductivity after the CTD is soaked
4. Filter (Section 5.4)
   (a) Low-pass filter temperature and conductivity with a two-way (i.e., zero-phase) 3-point triangular window
5. Align (Section 5.5)
   (a) Delay conductivity by 0.33 s (2 scans @ 6 Hz)
   (b) Advance oxygen by 3.0 s (18 scans @ 6 Hz)
6. Descent rate filtering / Loop Edit (Section 5.6)
   (a) Flag all sensor data when descent rate is less than 0.4 m/s and when acceleration is lower than -0.1 m/s^2

7. Derived variables (Section 5.7)
   (a) Practical Salinity using filtered and aligned conductivity and temperature. Ignore RBR's calculation.
   (b) Depth
   (c) Oxygen concentration in units of ml/l or μmol/kg from oxygen saturation, but only after filtering temperature, salinity, and density to match the slow time response of the oxygen sensor
8. Bin average (Section 5.8)
   (a) Average data into depth or pressure bins
   (b) In coastal applications bins are typically 1 m wide, and centred on integer values (i.e., 1 m, 2 m, 3 m, ...)
   (c) In open ocean applications users may wish to use larger bins

1.3 Structure of this report

The document is organized as follows: Section 2 summarizes the instruments and sampling locations used in this report. Section 3 provides a very brief overview on the RBR conductivity, temperature, and pressure sensors. Section 4 discusses field deployment best practices. Section 5 describes how the post-processing steps and parameters were determined. Appendix A includes an example of how the processing steps would be implemented using the freely available Matlab toolbox RBRproc.

2 Instruments and sampling locations

RBR Limited, established in 1976 in Ottawa, Ontario, designs and builds a variety of oceanographic sensors including a series of CTD loggers that samples at a sufficient rate for water column profiling.

The processing recommendations made in this report were developed using RBR data collected mostly by the Hakai Institute. Hakai owns and routinely profiles with three RBR loggers: two XRX-620 (S/N 18032, 18066), and one Maestro (S/N 80217). A fourth instrument, an RBR Concerto (S/N 065679) was on loan from the Pacific Salmon Foundation in April 2015 for use in the Johnstone Strait program.

Clark Richards (DFO/BIO; formerly RBR) supplied profiles from a 12 Hz Concerto (rated to 2000 dbar) taken in the Coral Sea. Sarah Zimmerman and Humfrey Melling (DFO/IOS) provided profiles taken in the Canadian Arctic with four 6 Hz Concertos rated to 740 dbar (S/N 65578, 65639, 65579, 65636).

3 RBR CTD logger principle of operation

The instruments in this study measure conductivity, temperature, and pressure (CTD) at either 4, 6, or 12 Hz, and some are fitted with additional sensors to measure biogeo-

chemical parameters. The conductivity cell and the thermistor are physically separated on these instruments, which means that a parcel of water is sampled at different times by the conductivity and temperature sensors (Fig. 1). In 2016, RBR introduced a new generation of the RBR Duo, Concerto, and Maestro instruments. They feature a new conductivity cell, which was designed so that the thermistor is mounted on the conductivity cell itself. The hydrodynamics of the new cell facilitate laminar flow, as well. This updated configuration is expected to change the processing approach, and therefore some of the recommendations made in this report are not relevant to the newer generation of instruments (for example, conductivity and temperature alignment). Finally, unlike most Seabird CTD profilers, RBR profilers are not pumped. This has important implications for aligning the sensors and for the descent rate.

Most RBR CTDs can operate in two different modes. The first is a manual deployment, where the user can manually initiate logging before the instrument is placed into the water. The second is a threshold deployment, where the instrument initiates logging when a specific channel crosses a threshold defined by the user. This has implications for methods that might be used to remove atmospheric pressure (Sec. 5.3).

3.1 Conductivity

The conductivity sensor consists of a wire coil housed within a 5-cm diameter ceramic Delrin cylinder. Its sensing volume, extending far beyond the housing, is 20 to 30 cm in diameter, however the measurement is weighted more heavily around the centre of the coils. The conductivity measurement is thus a weighted spatial average of the sensing volume, which could affect the approach used to filter and align this sensor with the smaller, but slower, thermistor. Approximately 80% of the measurement is made within the ceramic tube, with the remaining 20% coming from the volume outside the cell. Additional details on RBR inductive conductivity cells including calibration can be found in Shkvorets and Johnson [2010].

The conductivity cell has a response time that depends on the flow rate through the cell, but it is generally believed to be shorter than the thermistor time constant (Humfrey Melling estimates 0.3 s). It is important to match the response of the temperature and conductivity sensors to prevent salinity spiking, which in the case of RBR profilers means "slowing down" the conductivity sensor. The relatively large sensing volume of the conductivity sensor, as opposed to "point" measurements made by the thermistor, means that the conductivity sensor acts somewhat as a spatial filter. Some argue that this ultimately makes it impossible to truly match the conductivity and temperature response, however the consensus is that some filtering and alignment considerations can at least improve the data (i.e., reduce salinity spiking). This will be discussed further in the alignment and filtering sections.

3.2 Temperature

The temperature sensor is a millimetre-sized thermistor encased within a glass bead, which is located inside a metal tube that protects the thermistor from varying ambient pressure. Its sensing volume is a few cubic millimetres. The time constant, defined here

as the e-folding time measured after the thermistor is plunged into a well-stirred bath (producing a step change in temperature), is typically about 0.6 s. It is possible that the time constant will be a function of descent speed.

3.3 Pressure

The strain gauge pressure sensor is located either on the sensor end cap or on the side of the logger. The pressure sensor response time is <0.01 s – effectively zero – meaning the pressure data do not need to be corrected for alignment or response time. RBR CTDs measure and report absolute pressure, which is the sum of sea pressure and atmospheric pressure.

3.4 Auxiliary sensors

Many RBR profilers are equipped with third-party sensors to measure, for example, turbidity, chlorophyll-a, photosynthetically active radiation (PAR), and dissolved oxygen. This report does not address data from these sensors because the processing would likely differ depending on, for example, the sensor manufacturer (e.g., Seapoint or Wetlabs chlorophyll-a fluorescence), and their data are not typically combined to derive other parameters in the same way salinity is calculated from temperature, conductivity, and pressure. Dissolved oxygen, on the other hand, requires special treatment, especially when deriving concentration from percent saturation because the results are sensitive to differences in sensor time constants (Sections 5.4 and 5.5).

4 Field use

Although this report is primarily focused on post-processing, data quality is highly dependent on proper CTD field protocol, therefore, we provide recommendations that will help ensure the collection of high quality data.

As described earlier, the RBR CTDs use an inductive conductivity sensor. A feature of this sensor is that it measures the conductivity in a 20 cm diameter sphere of sea water around the sensor. Conductive objects in this sphere will offset the measured conductivity. If a guard was installed by RBR or the user to protect the conductivity cell and thermistor, then the CTD must be calibrated with the guard in place. All other objects in the 20 cm field may change the calibration. If a bottom line and weight are used, it should be attached to a frame that is more than 20 cm away from the conductivity sensor. Such a line should be of non-metallic construction and thin as possible and should be attached to the bottom of the guard.

Before deploying the CTD, check for objects in the field of the conductivity sensor. Check the thin platinum wire thermistor for foreign objects. Make sure the clear acrylic pressure port on the sensor end is free of debris. Remove the cover from the dissolved oxygen sensor, and the fluorometer if present.

Lower the CTD into the water to initiate the 2 minute “soak”, which allows the instrument to thermally equilibrate to the water, and for any bubbles which might be

trapped near the sensors to escape or dissolve. Ensure that the water conditions are sufficient to initiate logging if the instrument is set to threshold mode. A common approach is to set the pressure threshold to the pressure expected at a depth of 2 m (i.e., 12 dbar). After 2 minutes, raise the CTD to near the surface, and begin the profile.

RBR CTDs are normally deployed either using a puller or using a mechanical winch. With a puller, if the rope is not spooled then the CTD will fall freely. Allow the CTD to free fall smoothly, and avoid rapid acceleration and deceleration. If the CTD is deployed using a mechanical winch, then lower at a rate of about 1 m/s. Lowering the CTD at an consistent speed of about 1 m/s is critical to avoid rapid acceleration during the deployment because an uneven descent rate will negatively impact data quality (Section 5.6).

5 Data post-processing

5.1 Correct for A2D zero-order hold

The analog-to-digital (A2D) converter on RBR instruments must recalibrate once per minute. In the time it takes for the calibration to finish, a sample is missed. The onboard firmware fills this missed scan with the same data measured during the previous scan, a simple technique called a zero-order hold. Zero-order holds were found in several Hakai instruments, and they are also known to occur in instruments used by the Pacific Salmon Foundations' Marine Survival Project.

A zero-order hold is easily identified by finding where neighbouring samples have the same value. However, some sensors do not contain holds, which implies that full scans are not necessarily held. Furthermore, different channels are held on different instruments, and there are even cases where some sensors are held for more than one point. For example, on the Pacific Salmon Foundation's RBR Concerto, S/N 065679, the pressure, sea pressure, depth, and temperature fields have zero-order holds, while dissolved O_2 does not. On this instrument, conductivity and chlorophyll-a have zero-order holds on the same scan, but also on the previous scan. On the Hakai RBR CTD S/N 080217, the temperature, chlorophyll-a, PAR, and turbidity fields have zero-order holds, while conductivity and dissolved O_2 do not.

It would be trivial to identify and fix the zero order holds if all sensors were held during a scan. Simply finding where consecutive pressure readings are the same would be sufficient. As pointed out earlier, in some cases, the hold for temperature and pressure occurs on the same scan, whereas the hold for conductivity began on the previous scan (Fig. 2). Thus, not only does each sensor need to be treated independently, the number of points to fix can also differ.

Before continuing with the following data processing steps, we recommend that users first test to see if the data has zero-order holds by plotting the time derivative of raw pressure. This will serve as a reference point for other channels. If the derivative shows a zero value at regular intervals then we recommend that the user calculate the derivative of other sensors (e.g., conductivity, temperature, turbidity, oxygen, PAR, and chlorophyll). The reason for using pressure as a basis for finding zero-order holds in other data is

that pressure increases in a predictable way during the cast, whereas is it possible, albeit unlikely, for temperature and conductivity to be perfectly uniform with depth (e.g., such as might be found in the winter surface mixed layer in temperate open ocean regions).

After identifying a hold, the user has a choice on how to fix it. We recommend that the zero-value hold be replaced either with a filler (e.g., `NaN`) or with an interpolated value calculated from the points surrounding the zero-order hold.

Finally, we wish to point out some anomalous behaviour in the pressure record of the Hakai RBR CTD S/N 080217. Pressure has a zero-order hold, as well as a noticeable problem on the scan after the hold such that the pressure sensor appears to overshoot the true value after the hold (Fig. 3). It is possible that other sensors demonstrate analogous behaviour, but this has not yet been investigated. If it exists, such an error might be difficult to find because other variables generally do not vary throughout the profile in a predictable, monotonic fashion. It is not clear at this time if this behaviour is limited to this instrument.

5.2 Data despiking

Despiking is the general term used to identify and subsequently correct or remove spurious data points. Spurious data are often "spiky", meaning that they differ significantly from neighbouring data. In Seabird's data processing suite this is referred to as "Wild Edit."

Median filters are commonly used to find spikes in data. One common algorithm is:

1. Create a smoothed time series with a median filter.
2. Subtract smoothed time series from original.
3. Calculate the standard deviation, s, of this residual.
4. Flag individual values lying outside of a defined tolerance level (e.g., $4s$)

In idealized cases, the median filter despiking easily identifies spurious data (Fig. 4). However, in actual applications it is not always clear whether the algorithm correctly identifies truly spurious data. For example, consider Fig. 5, which shows a fluorescence profile taken by Hakai staff on the BC coast on 09 Sep 2014. The 3-pt filter, which was very effective on our idealized signal, flags data that are clearly bad (note the spike at 30 dbar), but also data which is likely good (7 dbar).

Tests on conductivity show data despiking could be useful for flagging spurious density features which occur when the CTD momentarily reverses direction during a downcast (called "loops" by Seabird). However, analyzing for and removing these points is accomplished in the descent rate filtering step (Section 5.6). The despiking algorithm also finds conductivity regions that appear to be density inversions, however, whether inversions are realistic or not should be diagnosed with salinity and/or density. Despiking could also be used to remove salinity spikes from improperly aligned and matched conductivity and temperature data.

Ultimately it is up to the individual researcher to choose whether to apply a despiking algorithm. Median filtering algorithms are generally inappropriate for smoothly varying

data such as conductivity and temperature (the same is true for Seabird's algorithm). Properly aligning, filtering, and descent rate filtering are, in principle, better options to handle irregularities in conductivity and salinity.

5.3 Correction for atmospheric pressure

RBR CTDs measure and record total pressure, where total pressure is the sum of atmospheric pressure and sea level pressure. Atmospheric pressure must be removed from total pressure to obtain sea pressure, and sea pressure is required to calculate, for example, depth and Practical Salinity.

In the absence of independent measurements of atmospheric pressure, a common approach is to assume that it is 101.325 kPa (10.1325 dbar), which is the globally-averaged atmospheric pressure at sea level. However, atmospheric tides and synoptic weather cause sea level pressure to vary naturally by about ± 0.6 dbar, and the maximum difference between the highest and lowest sea level pressures ever recorded is 2 dbar. These changes are within the expected accuracy for a pressure sensor rated for coastal applications, which means atmospheric pressure fluctuations could be resolved with the CTD pressure sensor. The question then becomes: Is the atmospheric pressure reading from the CTD reasonable? Furthermore, pressure sensors often show hysteresis, which in this context means that the sensor could produce different values for the same actual pressure before and after a profile. If hysteresis is a problem, then it should be most noticeable in near-surface readings. Therefore, it was necessary to check whether the pressure sensor records consistent atmospheric values before and after the cast.

Data from the Hakai Institute on the BC Central Coast was used to test the viability of using RBR pressure data itself to estimate atmospheric pressure at sea level (SLP). The Hakai Institute maintains a meteorological station at sea level in Pruth Bay, Calvert Island. The instrument is a Campbell Scientific 106, which records barometric pressure at 5 min intervals with a claimed accuracy of $\pm$ 0.6 mbar ($\pm 6 \times 10^{-3}$ dbar). CTD profiles are collected almost daily from a hydrographic station about 2.5 km from the meteorological station. An estimate of air pressure from the RBR pressure sensor was obtained by choosing the minimum pressure for each profile, but only for those times when the conductivity was near zero to ensure the instrument was at the surface. A comparison of the two pressure estimates for a number of profiles is shown in Fig. 6. The comparison shows that the RBR estimate of atmospheric pressure is scattered around the 1:1 line with less than 0.25 dbar of scatter, with the error presumably caused by uncertainty in the RBR sensor. The manufacturer's specified error is 0.35 dbar for the Hakai instruments ($\pm 0.05\%$ of 700 dbar), which is slightly larger than the scatter in the regression. The positive correlation indicates that the CTD can measure SLP, but the fluctuations are large enough so that the measurements are generally not different from 10.1325 dbar.

Next we examine the pressure readings made before and after a profile to search for evidence of hysteresis. If hysteresis exists, then we need to determine whether the pre- or post-cast pressure reading is the best approximation of air pressure. Data from eight different instruments in three different regions were used to check for hysteresis. Table 1 summarizes the instruments used in the comparison.

The pre-cast and post-cast near-surface pressure values for the Hakai instruments are regressed in Fig. 7. The data lie scattered around the 1:1 line with less than 0.1 dbar of deviation, with a 0.02 dbar bias toward higher pressure before the cast. We note that the pre- and post-profile pressure readings from the Hakai profiles on the BC coast were taken while the instruments were submerged but near the water surface instead of in the air because these instruments do not initiate logging until they exceed a specific pressure threshold. At any rate, the bias and scatter in this regression is well within the pressure specification for the instrument, and generally smaller than atmospheric pressure fluctuations.

The Coral Sea in-air pre- and post-cast values are regressed in Fig. 8. The instrument used in this comparison was rated to 2000 dbar. The pre-cast pressures were always higher than the post-cast values by a median value of 0.04 dbar, while the maximum was 0.1 dbar. As with the comparison made using instruments rated for lower maximum pressures, it is important to note that the errors are well within the manufacturer's stated uncertainty of about 1 dbar (0.05% of 2000 dbar).

In summary, near-surface in-water pressure recordings compare favourably to nearby measurements made at a meteorological station. The scatter in this comparison falls within the stated uncertainty in the pressure sensors. This suggests that the CTD pressure sensor provides a reasonable estimate of air pressure, and that this can be used to remove the air pressure from total pressure. Finally, hysteresis is measurable but insignificant relative to the stated accuracy of the pressure sensor, meaning either the pre- or post-cast estimate is equally suitable.

Ultimately the errors caused by using the nominal atmospheric pressure instead of the local measured atmospheric pressure (whether measured by a CTD or a meteorological station), translate into small errors in salinity. A 1 dbar error will cause at an error in Practical Salinity of $\mathcal{O}(10^{-4})$ PSU, which is much smaller than the manufacturer specifications. The most important effect of incorrectly accounting for atmospheric pressure is when trying to accurately measure shallow depths.

Note on the temperature dependence of pressure

IOS scientists used four RBR Concertos in the Canadian Arctic Archipelago during the spring and summer of 2015. Two instruments had similar starting and ending surface pressures, however the other two had differences larger than the stated pressure accuracy (Table 1). The air-sea temperature differences were often very large; water temperatures ranged between -2 and 0°C, air temperatures were ≈-20°C, and the instruments were stored indoors at +20°C. The pre- and post-cast pressure differences may be due to how the pressure sensor's temperature is handled in the pressure calculation.

The stated pressure accuracy is ±0.4 dbar for these four instruments based on ±0.05% accuracy of 740 dbar full scale. Two of the loggers (S/N 65578, 65639) provided surface pressures from the start and end of the casts within 0.2 dbar (Fig. 9), however the other two loggers (S/N 65579, 65636) had pressure differences ranging from 0.3 to 1.2 dbar depending on the cast. For the two instruments with larger pressure differences the ending pressure was always lower than the starting pressure.

A pressure dependence on temperature was clearly seen in the three instruments used

in very cold air temperatures when the instruments were removed from their protective environment and exposed to cold air before the cast. Interestingly, the direction of the dependence varied depending on the logger. For S/N 65639, an in-air temperature change of -15°C led to in-air pressure change of -0.13 dbar (+0.1 dbar/10°C). For S/N 65636, a change of -40°C led to an in-air pressure change of +1.2 dbar, and for S/N 65579, a change of -10°C led to an in-air pressure change of +0.6 dbar (-0.45 dbar/10°C). When the second two instruments were put into the relatively warmer water, the pressures of both decreased, consistent with their temperature dependence.

Effects of water freezing around the sensors cannot be ruled out, and a couple of the instruments described above were only used for 3 and 4 casts.

These results indicate that when working in extreme temperatures, standard practices of data processing and expected accuracy statements may need to be changed.

The variable dependence of pressure on temperature arises because of how this issue is handled differently between the model generations. Most instruments using the musical names (e.g., Concerto), would have pressure compensation via a thermistor in the pressure sensor, while older instruments either used the external "marine" thermistor or compensating resistors built into the pressure transducer (e.g., old Concertos or XRX-620s). The result for the instruments using compensating resistors is that the pressure calibration is most accurate at the calibration temperature (approximately 20°C), but may deviate some for different temperatures.

5.4 Low pass filter

Low pass filtering conductivity, temperature, and pressure data is used to 1) match sensor time constants, 2) smooth high frequency noise and, in some instruments, 3) remove quantization errors in pressure sensors. Each of these will be discussed here. Of course data from any sensor can be filtered, however in this report we discuss conductivity, temperature, pressure, and O_2.

The primary reason to filter temperature and conductivity is to match their response times. The rate at which conductivity and temperature sensors respond to impulsive signals is quantified by a time constant. In the case of RBR instruments, the conductivity sensor has a faster response, and therefore it needs to be "slowed down" to match the response time of the temperature sensor. Oxygen sensor time constants are longer than both temperature and conductivity. Matching the sensor response times of conductivity and temperature is necessary to reduce salinity spiking, and matching temperature and salinity to dissolved oxygen percent saturation is necessary to calculate dissolved oxygen concentration.

Low pass filters are also applied to CTD data to smooth undesirable high frequency noise. For example, noise might be introduced into the temperature sensor because of the hydrodynamic turbulence caused by the conductivity cell.

The pressure sensor on RBR profilers has a fast response time of less than 0.01 s, and while it is used to calculate practical salinity, it is not necessary to slow down the response by filtering. However, there are times when it is useful to filter pressure. The first is that pressure should be filtered when it is used to calculate the descent rate, because taking the derivative of a time series tends to amplify noise from the raw time series. Filtering

pressure will reduce the noise and produce a smoother descent rate. The second case is when a pressure sensor with a very deep rating, say 1000 dbar, is used in shallow water. The precision and accuracy of a pressure sensor depend on its maximum depth rating (i.e., the full scale reading). For example, a 1000 dbar sensor with an accuracy of 0.05% translates into a potential error of up to 0.5 dbar. If this is used in a shallow area, the relative error, in terms of the (potential) bias compared to the profile depth, could be large. Low-pass filtering can be helpful in this case to remove random errors, but the bias will still remain.

By way of comparison, Seabird generally recommends filtering pressure for some of their instruments (e.g., SBE 19+) to remove quantization errors. RBR sensors, while also using strain gauge sensors, do not appear to suffer from such errors. The difference is in how the signals are digitized and recorded on the instrument.

Finally, we will need to filter temperature and salinity with a long time constant filter to match them with the dissolved oxygen sensor response. This is necessary because oxygen saturation is required to convert from the measurement of relative dissolved oxygen concentration (i.e., percent saturation) to an absolute concentration, and oxygen saturation depends on salinity and temperature.

5.4.1 Filter type

In idealized cases, the task of matching time constants and phase responses relies on recursive filters, which are a type of infinite impulse response (IIR) filter. Recursive filters have a time history built in to model the response of a sensor to changes in the environment. Applying a recursive filter to a rapidly changing "step" signal will 1) smooth the step and 2) change the phase. Schmitt et al. [2005] recommend this type of filter because it produces the required phase delay, which is to say it lags the signal to account for a finite response time.

SeaBird uses an IIR filter, however whether it is a Butterworth filter or something else is unclear. It is a bilinear filter, which is ideal in cases where the sample interval is near the response time [Schmitt et al., 2005]. In principle, the filter produces the necessary phase lag, however Seabird's filter is applied to the data in both directions (in analogy with `filtfilt.m` in Matlab). Running the filter in both directions produces two effects: 1) the amplitude response is smoothed more than a single pass with the filter, and 2) the phase shift is zero. The zero phase shift response is not realistic, however, Seabird has presumably chosen to address the phase shift issue with the alignment step, whereby the time series of a particular sensor is advanced or delayed in time. Sensor alignment is addressed and also recommended by Schmitt et al. [2005].

Oceanographers commonly use moving-average type filters, most of which are considered Finite Impulse Response (FIR) filters. The most common FIR filter is the moving average, or boxcar.

An informal survey of the workshop participants showed that users rely on different filters. For example, Humfrey Melling at IOS recommends using a running 3-point triangular window to smooth a 6 Hz conductivity signal. Clark Richards at BIO tailors the filter depending on the nature of the T/C data itself. In some cases, it makes sense to explicitly match time constants and adjust the phase response (e.g., with a recursive

phase-forward filter), while in others it makes sense to simply smooth high-frequency variations with a simple running mean.

Does the filter type (FIR vs. IIR) matter for the environments sampled by RBR CTDs? To get some understanding of the difference between FIR and IIR filters, Fig. 10 and Fig. 11 provide a comparison of the IIR single-pole type filter to a FIR 3-pt triangular window. In both cases the filter was applied in forward and reverse directions to keep the phase shift at zero (using the Matlab function `filtfilt.m`). The 1st-order Butterworth filter had a cutoff frequency of 1 Hz, where the cutoff frequency is the frequency at which the signal is attenuated by 3 dB.

In this example, the Butterworth cutoff frequency was chosen manually to approximate the 3-point triangular filter (the cutoff frequency can be fine-tuned to more closely match the 3-point curve). While there are physical arguments that support the use of a recursive filter (e.g., the phase delay), it is clear from this simple example that difference between the filters is minimal if they are applied in both directions. One must still account for phase delays, which in principle could be achieved by forward filtering only, however this can be introduced during the sensor alignment correction (Section 5.5).

Therefore, under normal circumstances (e.g., coastal waters or noisy sensors), use of a simple FIR filter, such as a running mean (perhaps weighted with, for example, a Hanning or triangular window), applied in the forward and reverse directions, is sufficient. While the IIR-type filter used by Seabird was designed to emulate the response of a real sensor, most oceanographers are more familiar with FIR filters. The difference between the filters is not large enough to warrant using the more sophisticated (yet realistic) IIR filters. To further ensure that the temperature and conductivity time constants are closely matched, the same filter should be applied to temperature.

5.4.2 Dissolved oxygen

Finally, in order to calculate O_2 concentration from O_2 percent saturation, it is necessary to compute the O_2 saturation value, which a function of temperature and salinity. Thus temperature and salinity should be filtered to match the relatively slow response time of the dissolved oxygen sensor. The filter time constant or window length will depend on the time constant of the particular oxygen sensor, but a rough guideline might be found by considering the lag needed to align the O_2 sensor to the pressure and temperature sensors (Section 5.5).

5.5 Sensor alignment

Aligning the sensors on a CTD accounts for two different factors. The first is that each sensor encounters a water parcel at a different time as the CTD moves through the water because of physical separation (different location on the instrument). The lag time depends on the separation and the descent speed because these factors determine the transit time of a water parcel between the sensors. The second is that the finite response time of a sensor causes a lag in the data because of the time it takes for it to equilibrate with its new surroundings. In principle, a well-designed filter could impart a phase change to account for the finite response time, however the approach usually

taken is to filter in such a way as to keep the phase at zero, and then shift the sensor in time. The use of sensor alignment to account for response time is especially important for dissolved oxygen.

5.5.1 Conductivity and temperature

Conductivity and temperature must be aligned to produce an accurate value of practical salinity. If the sensors are misaligned, then the salinity profile will contain small spikes because conductivity and temperature were not paired correctly.

For most RBR CTDs, the conductivity sensor encounters a parcel of water before the temperature sensor because of its physical location on the instrument, and because the field lines from the conductivity sensor extend some 20 - 30 cm into the water. Thus, it is necessary to delay the conductivity signal by a small amount. The temperature data is not shifted in time because the thermistor is physically located near to the pressure sensor.

In principle, one could calculate the appropriate delay for the conductivity sensor by simply dividing the distance between the conductivity sensor and the pressure sensor by the descent rate. However, the conductivity measurement is a weighted spatial average of a complicated sensing volume, and as mentioned earlier, we would also like to account for the response time of the "slower" temperature sensor. Fortunately, we can derive an empirical lag time by considering the quality of the derived salinity profile. In particular, we wish to minimize spurious salinity spikes that occur when temperature and conductivity are misaligned. Salinity spikes generally imply that there is an unstable density inversion in the water column, and while inversions can occur naturally, they are nearly always a consequence of sensor misalignment.

Figure 12 shows a select depth range of multiple profiles of salinity calculated from a single profile of conductivity and temperature. Each profile was computed with a different lag of conductivity relative to temperature. The profile was taken by the Hakai Institute on September 14, 2015, at station FZH08 on the British Columbia central coast. The descent rate ranged from 1.8 m/s near the surface to 1.4 m/s at depth. The optimum lag for conductivity in this example is in the range of -0.167 to -0.334 s (-1 to -2 scans at 6 Hz), where the negative sign indicates a time delay. The optimal lag produces a salinity profile, which has minimal spiking at steep temperature and conductivity gradients.

5.5.2 Dissolved oxygen

Alignment is particularly important for oxygen sensors because they have a much slower response time than temperature and conductivity.

To determine the appropriate lag time, we consider data from an JFE-Alec Rinko III oxygen sensor, which is the sensor used on multiple RBR loggers used by the Hakai Institute. These are fast response sensors designed specifically for profiling applications. The Rinko III is an optode-type sensor instrument that measures the changes in phosphorescence quenching phase shift of a substrate, caused by changes of oxygen partial pressure in the water. Oxygen partial pressure is related to in situ oxygen saturation (as a percentage) by dividing by the partial pressure of oxygen in the atmosphere (21 kPa).

JFE Alec does not provide a recommended advance time; however they JFE Alec state that the sensor response time is 0.9 s for a 90% change at a temperature of 25°C. This means that the sensor reaches 90% of the true value 0.9 s after being exposed to a step change in O_2. We assume that a lag time should be similar to the response time. It is worth noting now that this is a gas phase response, which means that the response time was derived by measuring how long it takes for the sensor to respond to a step change in gaseous O_2.

Two studies have been conducted to characterize the Rinko III response time. Sasano et al. [2011] conclude that 1 s is a reasonable value, while the more detailed study of Bittig et al. [2014] find that a reasonable response time based on field data is 4.7 s - substantially longer than 1 s. The longer response time is thought to be caused by fact that the oxygen measured at the optode foil must diffuse through a laminar boundary layer, which means that the response time is a function of the water flow rate past the sensor. Bittig et al. [2014] also determine that the response time is a function of temperature.

Given the large spread of response times found in these studies, a range of lag times were applied to a few of the Hakai Institute's O_2 profiles to determine an optimum lag. For simplicity, we seek a single lag value instead of trying to account for variations in flow rate (i.e. CTD descent rate) and temperature. We follow Seabird's recommendation to search for the lag that "collapses" the up and down casts on a T-O_2 diagram. In other words, when the lag is set correctly, O_2 will be paired to the correct temperature (and therefore pressure and time).

Figure 13 shows the T-O_2 relationship for a single profile taken on March 30, 2014, at Hakai station DFO1, for oxygen advance times of 1 s to 4 s in 1 s intervals. It is clear that an advance of 1 s (6 scans at 6 Hz) is not sufficient to collapse the up and down casts, whereas an advance of 2 or 3 s brings the O_2 up and down casts closer together. Finally, an advance of 4 s over-compensates.

In addition to T-O_2 plots, O_2 profiles were plotted for both aligned and unaligned profiles to gain an intuitive understanding of the O_2 sensor advance times. Somewhat counter intuitively, we argue that the optimal advance is not the one that makes the up and down casts agree perfectly because the hydrodynamic wake generated by the CTD. The wake, in combination with the sensor location on the instrument, will cause an inherent mismatch in water properties between up and down casts. For example, depth profiles of temperature show a roughly 2 m difference between up and down casts. If we assume the downcast represents the actual temperature profile because the sensor is encountering undisturbed water, then the up/down mismatch must be caused by the upcast, which, according to the wake explanation, is because the CTD is measuring disturbed water caught in its wake. Thus, we seek to delay the O_2 signal by an amount that produces a depth difference equal to what is seen in temperature - roughly 2 m. With the above in mind, a plot of the up and downcast data shows that a 3 s advance (Fig. 14) causes an up/down cast depth offset of about 2 m.

The 3 s advance found here is longer than JFE Alec's quoted value and the Sasano et al. [2011] study, but it is roughly consistent with the findings of Bittig et al. [2014]. The longer time found in our study is presumably due, at least in part, to the much cooler waters on the BC coast in comparison to the 25°C temperature at which the manufacturer specification was made. The 3 s advance found for the profiles in Fig. 13

was determined by considering a profile made in 7°C water. As a quick test to check if the temperature dependence is important under the range of water temperatures observed on the BC coast, consider an O_2 profile from Pruth station on August 10, 2015, in which the temperature increases from 16°C near the surface to 11°C at 20 m. The optimum O_2 advance for this warm layer was found to be about 2 s, consistent with the expectation that the response time decreases with increasing temperature.

Finally, we point out that Bittig et al. [2014] found that the flow rate past the sensor had a significant impact on the time constant. The flow rate dependence was stronger than the temperature dependence. We don't address this issue here, however, the flow rate sensitivity means that users should strive for consist descent rates in the field to simplify data processing.

5.6 Descent rate filtering

Large seas will cause the CTD descent rate to vary as the boat heaves, particularly when the CTD is being lowered by a taut line (instead of falling freely). In the case when the CTD slows, stalls, or reverses, water entrained in the CTD frame or rosette continues downward and is sampled by the instrument. This is called the wake effect. This water likely has different properties than its surroundings, which will contaminate the sample.

To examine the impact of inconsistent descent rates on the CTD data, we calculated the first derivative of density from 117 profiles that were collected at 5 stations (DFO2, FZH01, HKP01, PRUTH, and QCS01) on the British Columbia central coast from 2012 - 2014. Unless in exceptional circumstances, density increases with depth meaning negative values could indicate the wake effect. Results suggest that there were density inversions at all positive descent speeds (i.e. the downcast), which indicates that descent speed alone is not a good indication of the conditions that create density inversions due to the wake effect (Fig. 15).

Next, we examined the first derivative of descent speed to get an indication of how much the CTD is accelerating or decelerating (Fig. 16). Results indicate that density inversions are normally correlated with times when the CTD decelerates, though, since about half of the data are associated with some deceleration, deceleration on its own is not a good metric for diagnosing the wake effect. When the descent speed and deceleration were jointly examined for the density inversions, it was found that 21% - 100% of the density inversions were associated with a descent speed of less than 0.4 m/s and a deceleration of less than 0 m/s^2, while 1% - 8% of the density inversions were associated with a descent speed of less than 0.4 m/s and an acceleration less than -0.1 m/s^2 (not shown).

To estimate the amount of data that would be removed from different loop edit criteria, the percentage of data that had density inversions greater than 0.01 kg/m^3 were calculated. Then the percentage of data that would be removed with a strict (descent speed less than 0.4 m/s and acceleration less than -0.1 m/s^2) and lenient (descent speed less than 0.4 m/s and acceleration less than 0 m/s^2) loop edit criteria was calculated (Fig. 17). It was found that the number of density inversions ranged from 0.6% - 2.3 % per station. When the lenient criterion was applied, 0.6% - 2.5 % of the data would be removed. When the strict loop edit criterion was applied, 0.1% - 0.6 % of the data would

be removed. To minimize data loss while correcting for the wake effect, we recommend that data where the descent speed is less than 0.4 m/s and acceleration less than -0.1 m/s^2 are removed.

Low descent rates necessarily occur near the surface just as the CTD begins to descend after the soak period, and also at the end of the downcast near the bottom. The descent rate threshold alone does not necessarily flag low descent rate values because of the extra requirement that the deceleration rate must exceed a threshold. The threshold values of descent rate and acceleration rate are somewhat conservative in the sense that very few data points are flagged. However, a researcher may wish to consider implementing a routine that relaxes the threshold criteria near the bottom and near the surface, especially if, for example, acceleration rate was not considered.

5.7 Derived variables

In this step standard routines are employed to calculate a range of useful oceanographic variables such as salinity and depth from measured quantities (typically temperature, conductivity, and pressure). There are dozens of variables that can be derived from temperature, conductivity, and pressure, although many are relevant for only a small number of specialized purposes. Algorithms to compute many of the variables have been developed and ported to a number of programming languages (TEOS-10 Gibbs Seawater toolbox). Here we discuss just two quantities, Practical Salinity and dissolved oxygen concentration.

5.7.1 Practical Salinity

Practical Salinity is important to mention primarily because users are advised to discard any salinity variable computed by the RBR logger because it would have been made before the conductivity and temperature were properly filtered and aligned.

5.7.2 Dissolved oxygen concentration

The fundamental and relevant dissolved oxygen quantity is the actual concentration of oxygen, which is commonly expressed in units of ml/l or μmol/kg, whereas the Rinko III dissolved oxygen sensors (and other optodes) measure the percent oxygen saturation. As discussed in Section 5.5.2, the concentration of oxygen can be calculated by multiplying the percent oxygen saturation by the saturation level (also called the oxygen solubility).

As with salinity, it is important to note that oxygen concentration, if output by the optode or RBR logger, is typically an approximate value because dependence of oxygen solubility on salinity has not been considered. If, by chance, salinity was considered by the logger firmware or Ruskin, it is still advisable to recalculate oxygen saturation level because the time constants of the conductivity, temperature, and oxygen sensors must be matched.

5.8 Bin averaging

Bin averaging is a method that places the sensor measurements onto (often) regular and standardized depth, pressure, or time values. This reduces high frequency variability at the expense of resolution. Data can be binned according to pressure, depth, or time.

Bin width and spacing are both (nearly) universally chosen to be 1 m in coastal waters. Most RBR CTDs sample at a frequency of 6 Hz, and at a descent speed of 1 m/s, bins 1 m in width generally contain the average of 6 samples. Typically, the first bin is centred on 1 m. Therefore, the first bin contains the average of all data occurring between depths of 0.5 m to 1.5 m, the 2 m bin contains the average of all data occurring between depths of 1.5 m and 2.5 m, and so forth until the end of the profile. Note that, in this particular case, the shallowest bins excludes data from depths shallower than 0.5 m. In general, this is a positive side effect because near-surface data are often of questionable quality.

Alternative methods for bin averaging include the use of overlapping bins, where the width of each bin is greater than the bin spacing. One may also choose to window the data, placing more emphasis on the data occurring near the bin centre. Other possibilities include methods which produce bin estimates with less bias, which occur in cases when, for example, the unbinned data is not spaced equally in depth. The LOESS (locally weighted scatterplot smoothing) approaches could also be applied in this context.

6 Conclusion

Application of the post-processing steps presented in this report will significantly improve the quality of profiles made by RBR loggers, with a "cleaner" salinity profile being the most important result. Two different generations of RBR conductivity sensors exist; the steps here are most relevant for the now discontinued model which has the thermistor mounted on the pressure case and the cylindrical black or gray conductivity cell.

A correction for the thermal inertia of the conductivity cell was not addressed here [Lueck, 1990]. The conductivity cell exchanges heat with the ambient water if it moves through temperature gradients. The heat exchange changes the water temperature of the sensed water, and thus its conductivity. The resulting impact on salinity can be significant in regions with strong temperature gradients.

RBR is working to characterize the thermal inertia of its conductivity cells, and as of late 2016 some progress has been made on deriving a correction formula.

Acknowledgements

We would like to acknowledge the Hakai Institute and RBR for supporting this work, and the Institute of Ocean Sciences for hosting the workshops.

Owner/Region	CTD Model & Serial Number	Maximum pressure rating [dbar]	Stated Accuracy [dbar]	Cast depth [m]	Comparison to met station P [dbar]	Difference between pre- and post-cast [dbar]	Approx. water temperature [°C]
Hakai, Coastal BC	XRX-620, S/N 18032	700	0.35	75	±0.25	±0.05	N/A
	XRX-620, S/N 18066	700	0.35	75			
	Maestro, S/N 80217	1000	0.50	75			
RBR, Coral Sea	Concerto,S/N 65583	2000	1.00	2000	N/A	-0.04	N/A
IOS, Coastal Arctic	Concerto,S/N 65578	740	0.37	50	N/A	0.2	-1
	Concerto,S/N 65639	740	0.37	50			
IOS, Coastal Arctic	Concerto,S/N 65579	740	0.37	50	N/A	-0.3 to 1.2	-1
	Concerto,S/N 65636	740	0.37	50			

Table 1: Summary of viability study for the use of CTD pressure to estimate and remove the atmospheric pressure from total pressure.

Figure 1: Photo of an RBR concerto logger with the thermistor mounted on the CTD pressure case, and the old generation of conductivity cell (RBR Ltd).

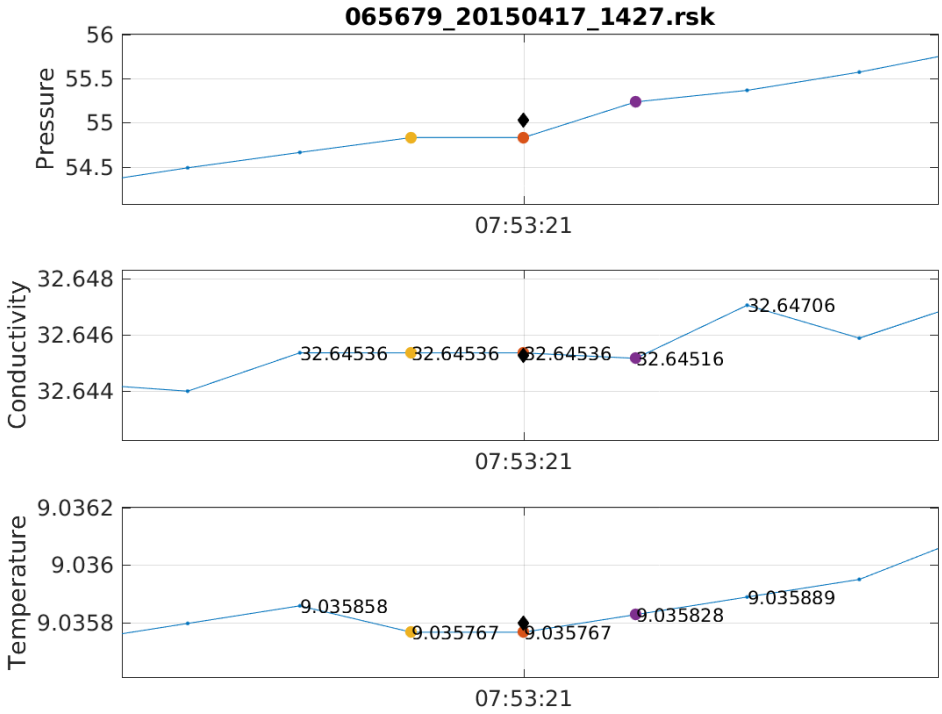

Figure 2: Time series illustrating a zero-order hold scan (orange dot) for RBR CTD S/N 065679. The yellow and purple dots are the nearest surrounding points. In this example the black diamond represents the replacement value. Conductivity stays constant for three consecutive values, including the point before the hold.

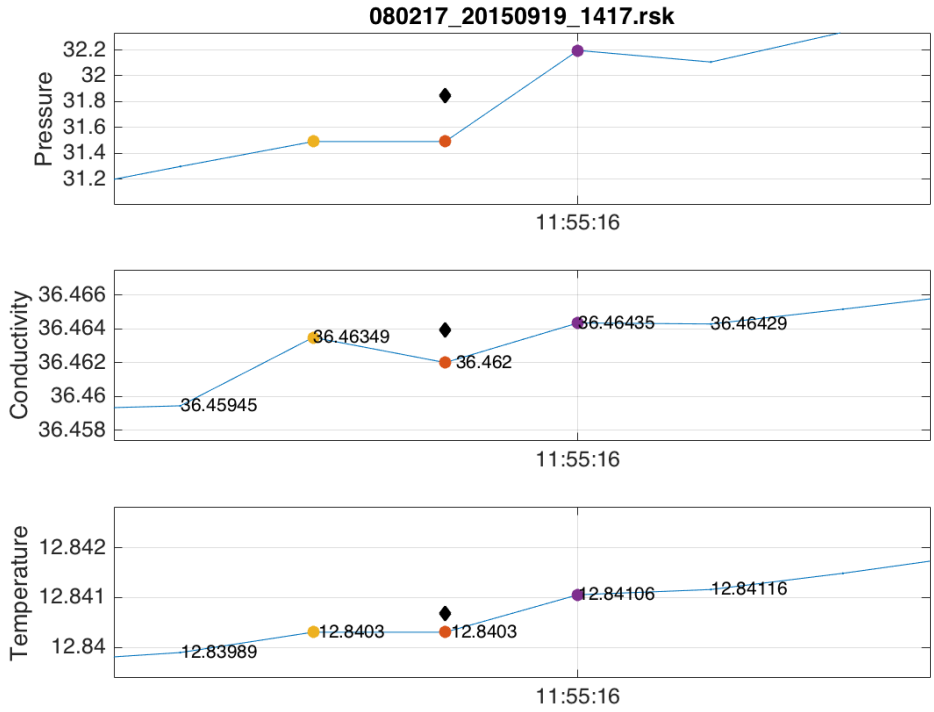

Figure 3: Time series showing 6 scans of pressure, conductivity, and temperature for RBR CTD S/N 080217. The pressure reading following the hold appears to overshoot its true value. Conductivity does not have a zero-order hold, while temperature does.

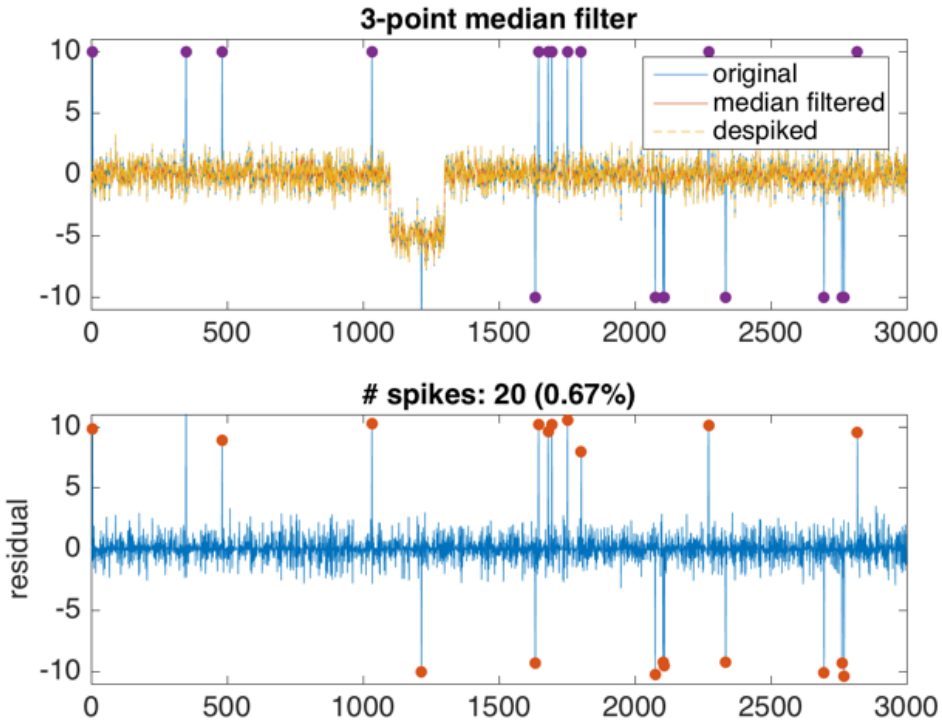

Figure 4: The upper panel shows a synthetic test case for the 3-point median filter despiking algorithm. The signal consists of white noise ($\sigma = 1$) centred on 0, 20 single-point spikes with an offset of $\pm$ 10, and a short section with a DC offset of -5. Data lying outside of $3s$ were flagged.

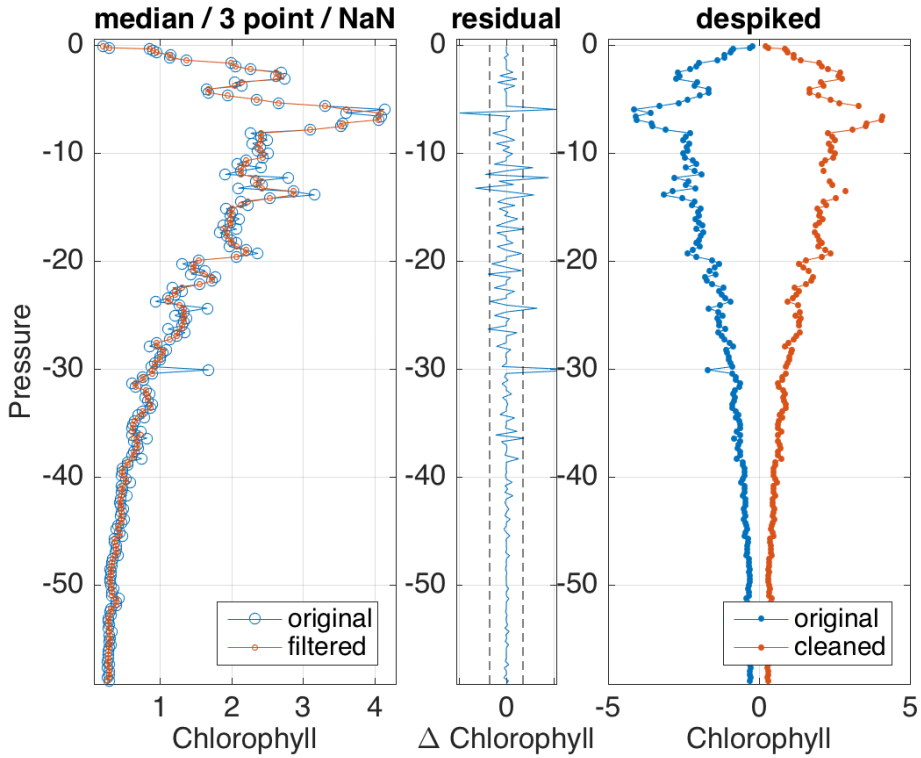

Figure 5: The panels from left to right are: raw and filtered chlorophyll-a fluorescence, residual profile (raw - filtered), and the original and "cleaned" profiles. The $\pm 4s$ threshold levels are shown by the dashed lines. In this example, residual values outside of the $4s$ threshold are flagged as bad.

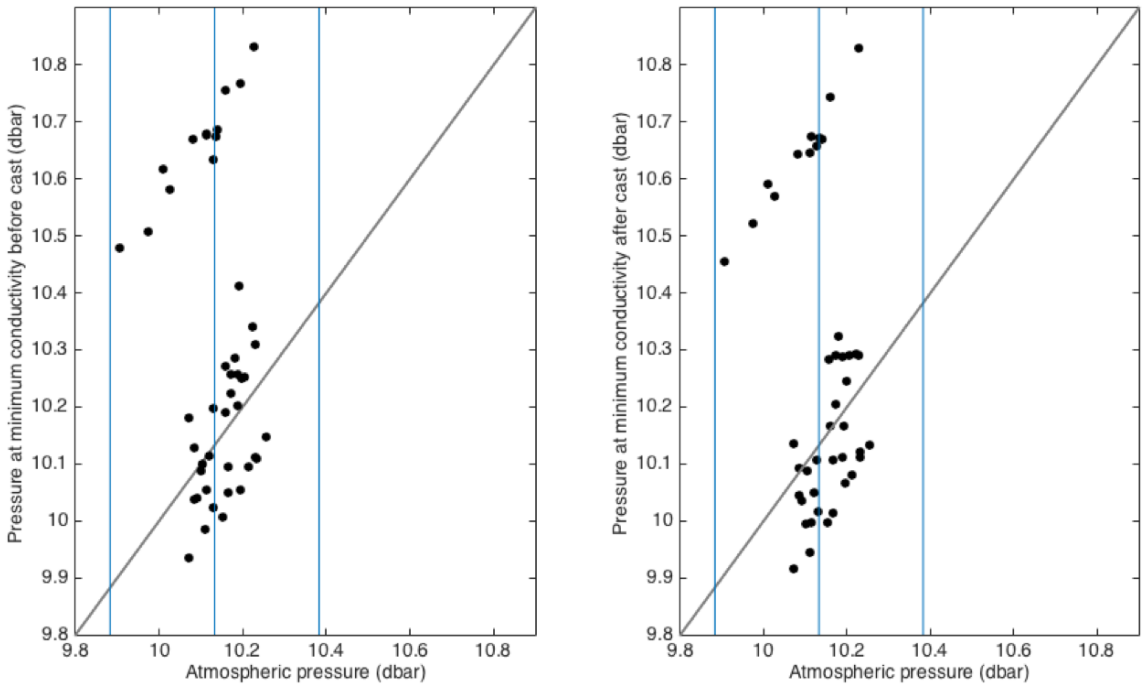

Figure 6: Comparison of atmospheric pressure measured at a Hakai meteorological station to CTD in-water near-surface pressure readings in water before the cast (left panel) and after the cast (right panel). The solid line represents x=y. The anomalously high CTD readings were later found to be caused by a faulty sensor.

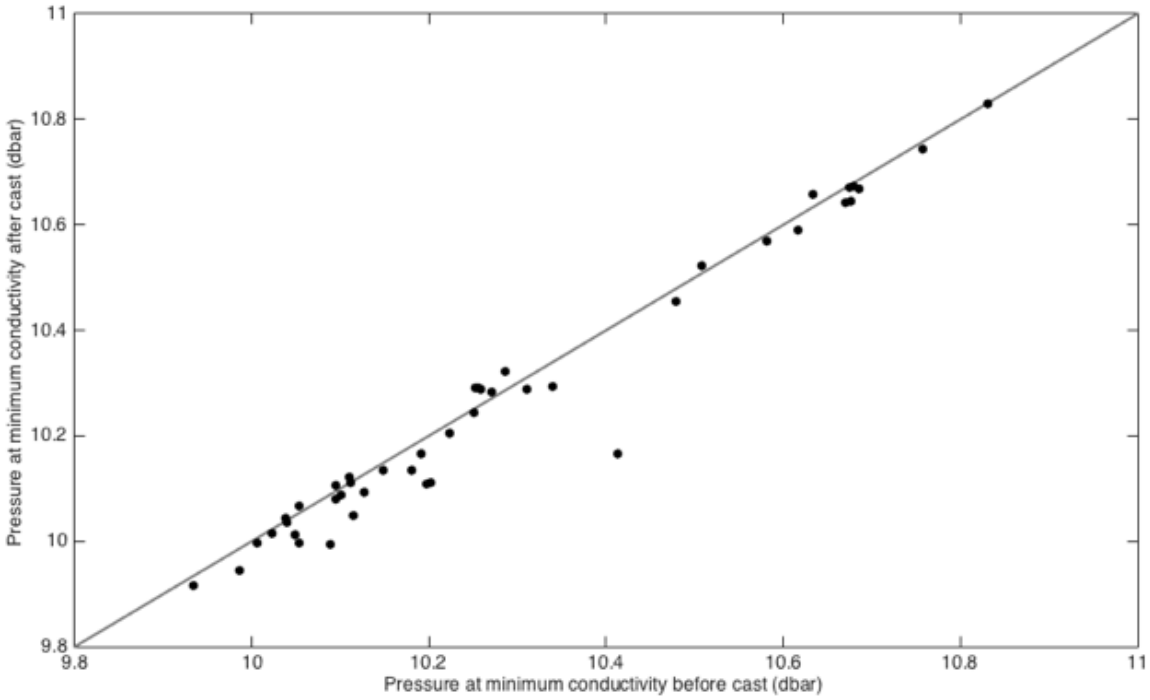

Figure 7: Comparison of surface pressure data collected after the soak (horizontal axis) and at the end of a cast (vertical axis) from a station on the British Columbia central coast. The solid line represents x=y.

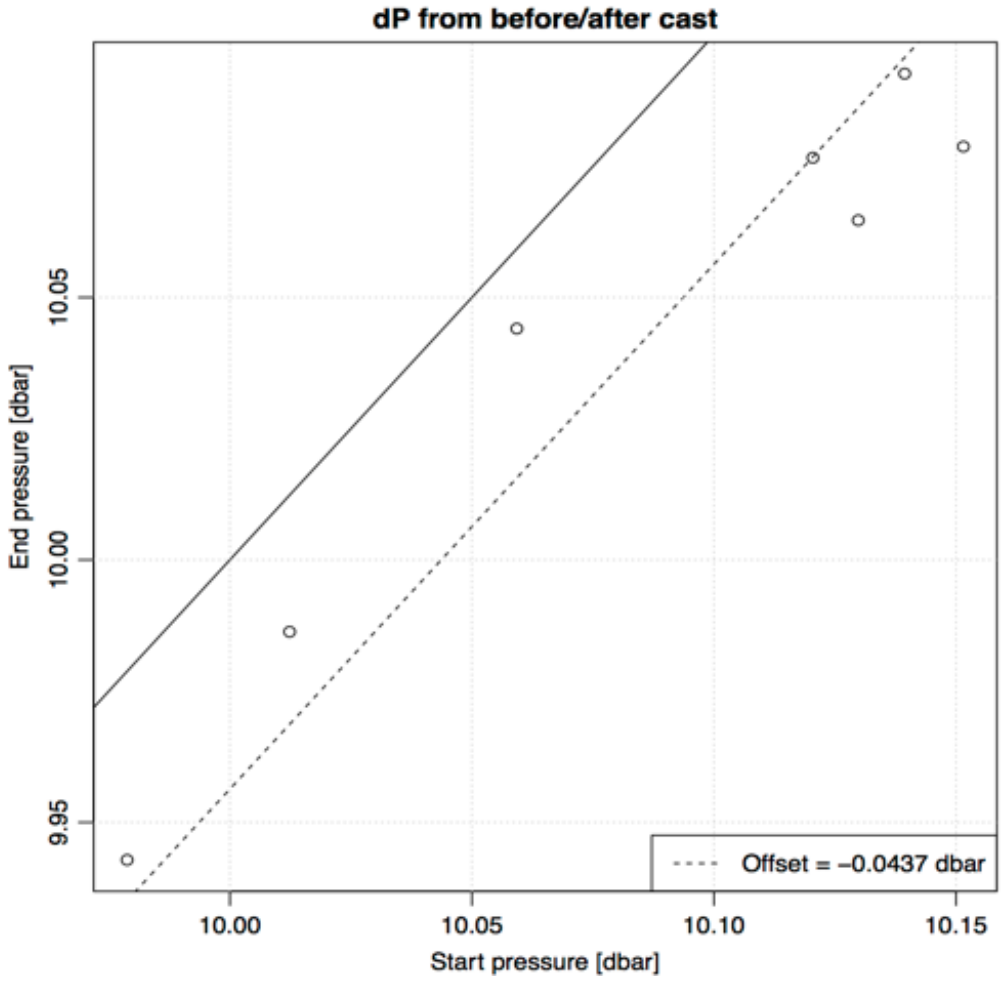

Figure 8: Comparison of in-air pressures collected immediately before and after a series of casts to 2000 dbar in May 2015 off of Eastern Australia in the Coral Sea. Note the offset of approximately 0.04 dbar, well within the stated accuracy of 1 dbar (0.05% of 2000 dbar). The solid line represents x=y.

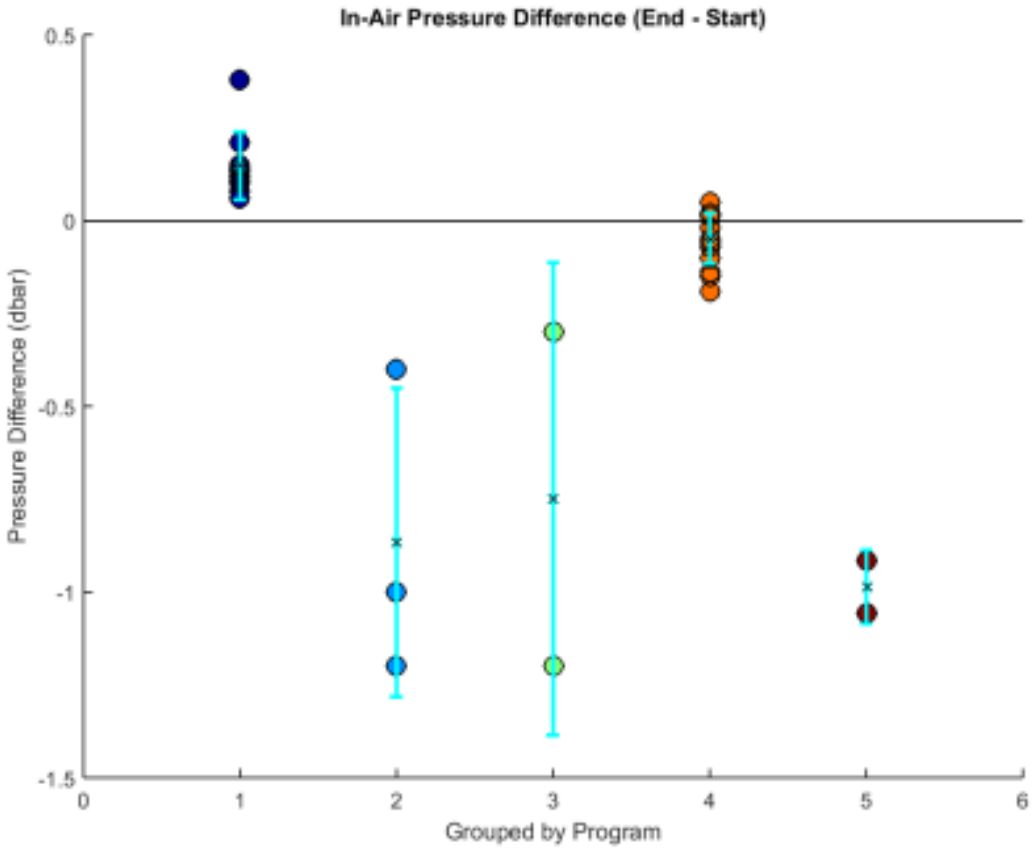

Figure 9: Boxplots of pre- and post-cast in-air pressure difference from profiles taken in summer 2015 on the Canadian Arctic shelf.

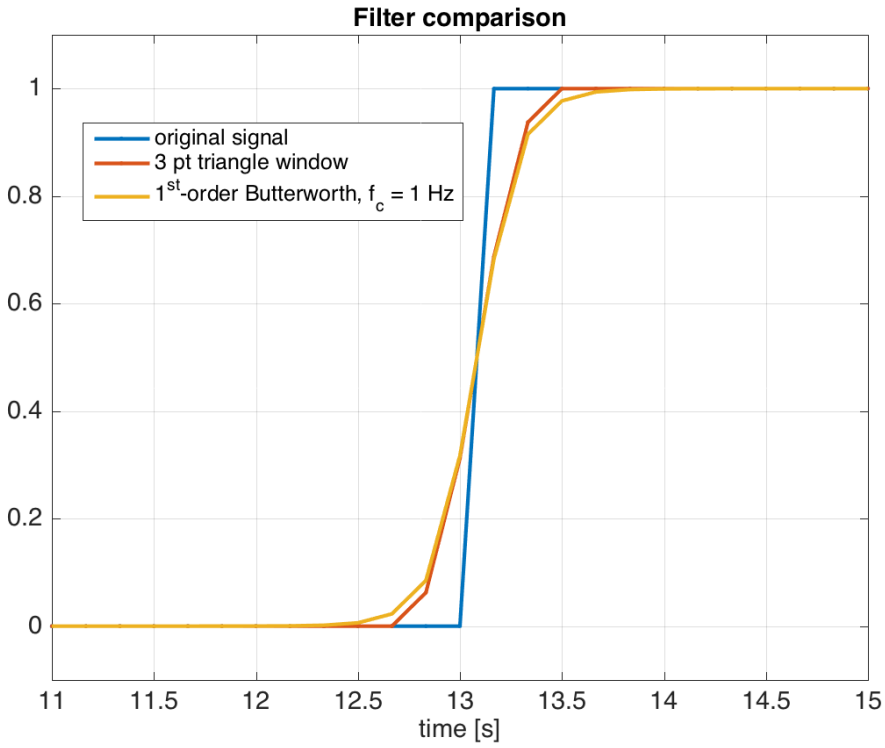

Figure 10: Comparison of filter performance for a 6 Hz step change signal. The filters were applied to the signal twice, once in the forward direction, and once in the reverse direction, to produce a filtered signal with zero phase shift.

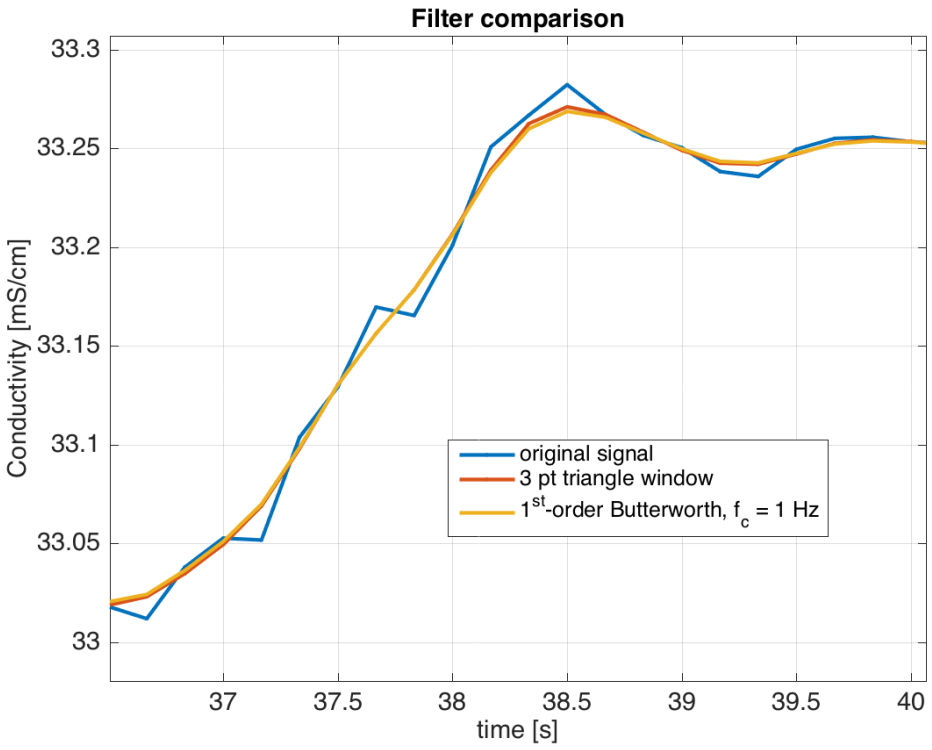

Figure 11: Filter comparison on a time series of 4 s of measured conductivity.

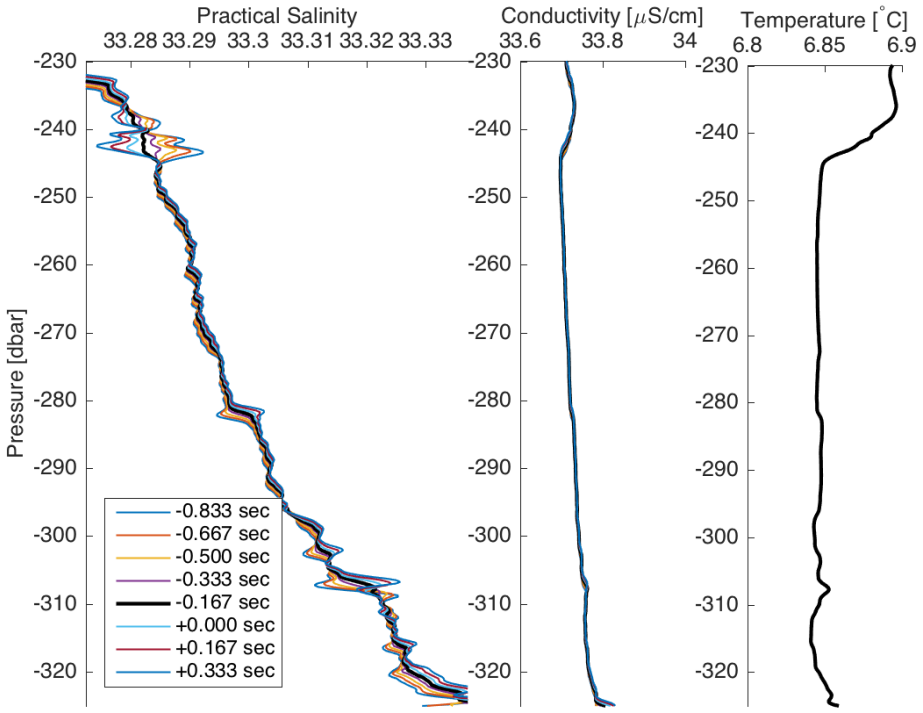

Figure 12: Profiles of Practical Salinity for a range of conductivity lag times. Negative lags constitute a time delay, while positive values indicate an advance. Conductivity and temperature profiles are shown for comparison. The CTD descent rate was 1.4 m/s through this section of the profile.

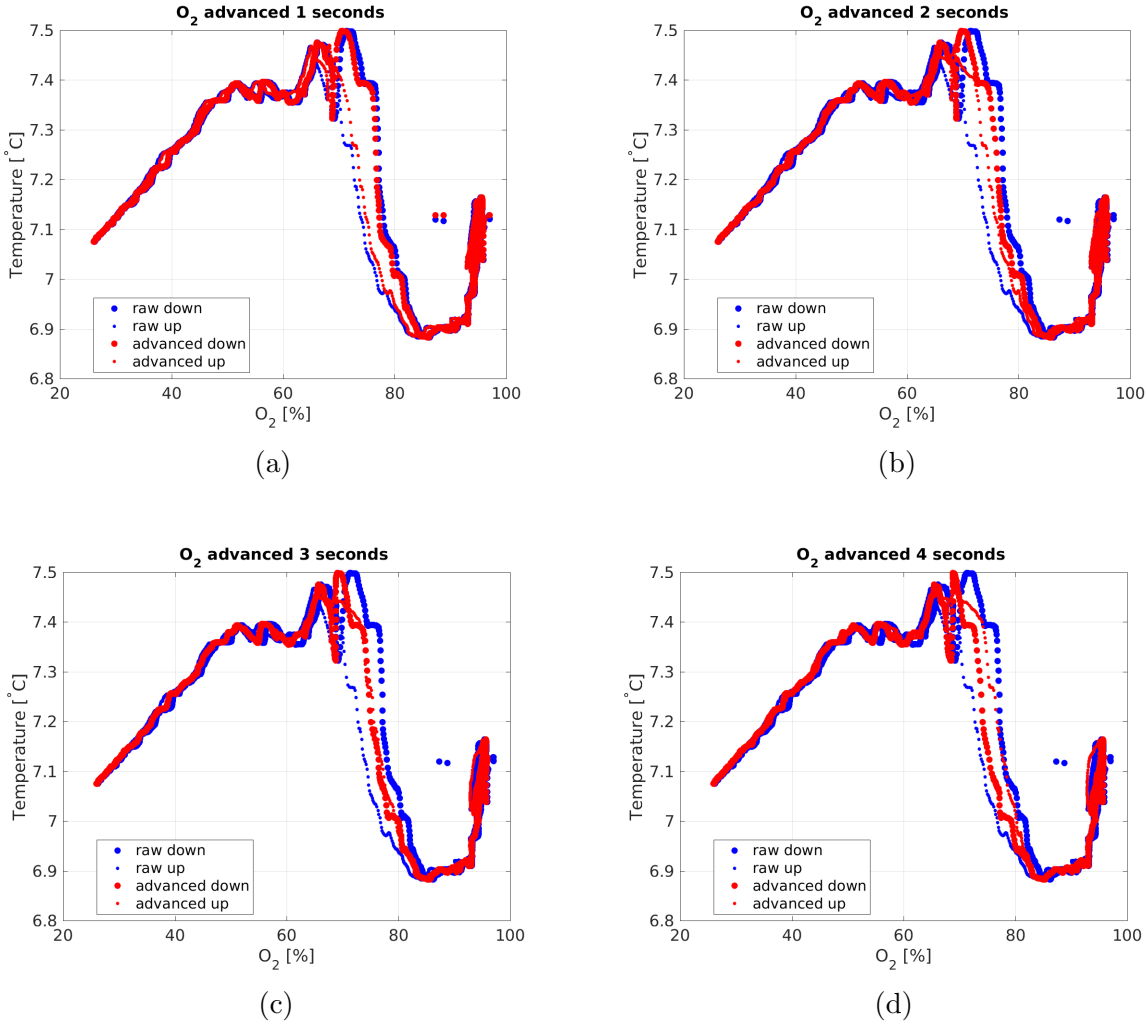

Figure 13: T/O_2 plots for oxygen sensor advance times of (a) +1 s, (b) 2 s, (c) 3 s, and (d) 4 s. The profile was obtained on March 30, 2014, at station DFO1.

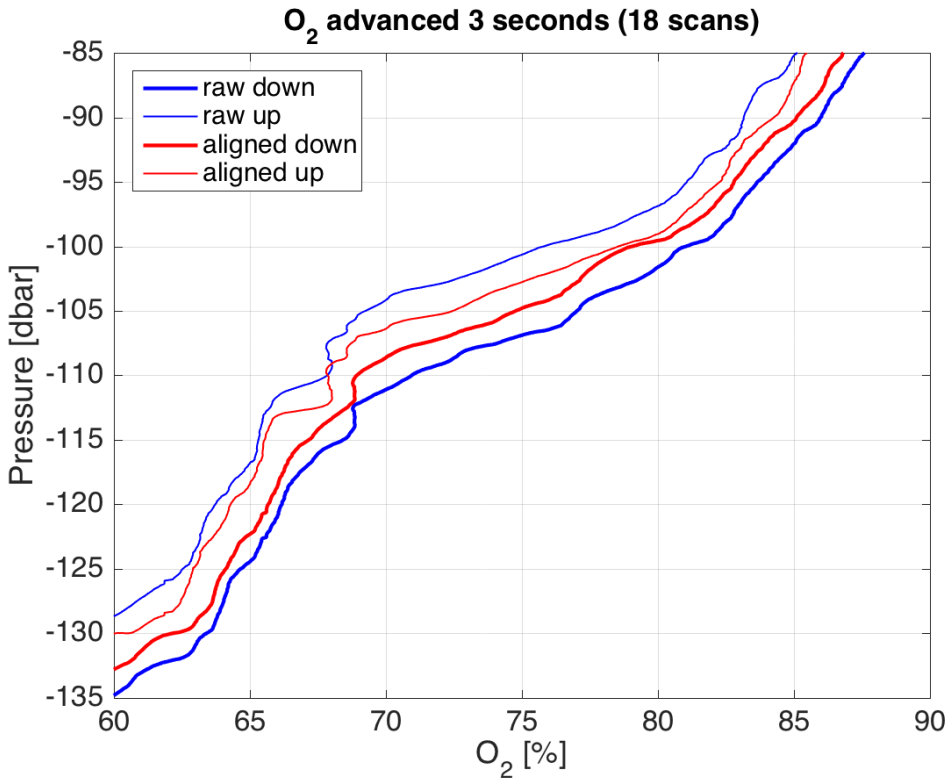

Figure 14: Section of an O_2 depth profile obtained on March 30, 2014, at station DFO1 (same profile shown in Fig. 13). O_2 was advanced by 3 s (18 scans).

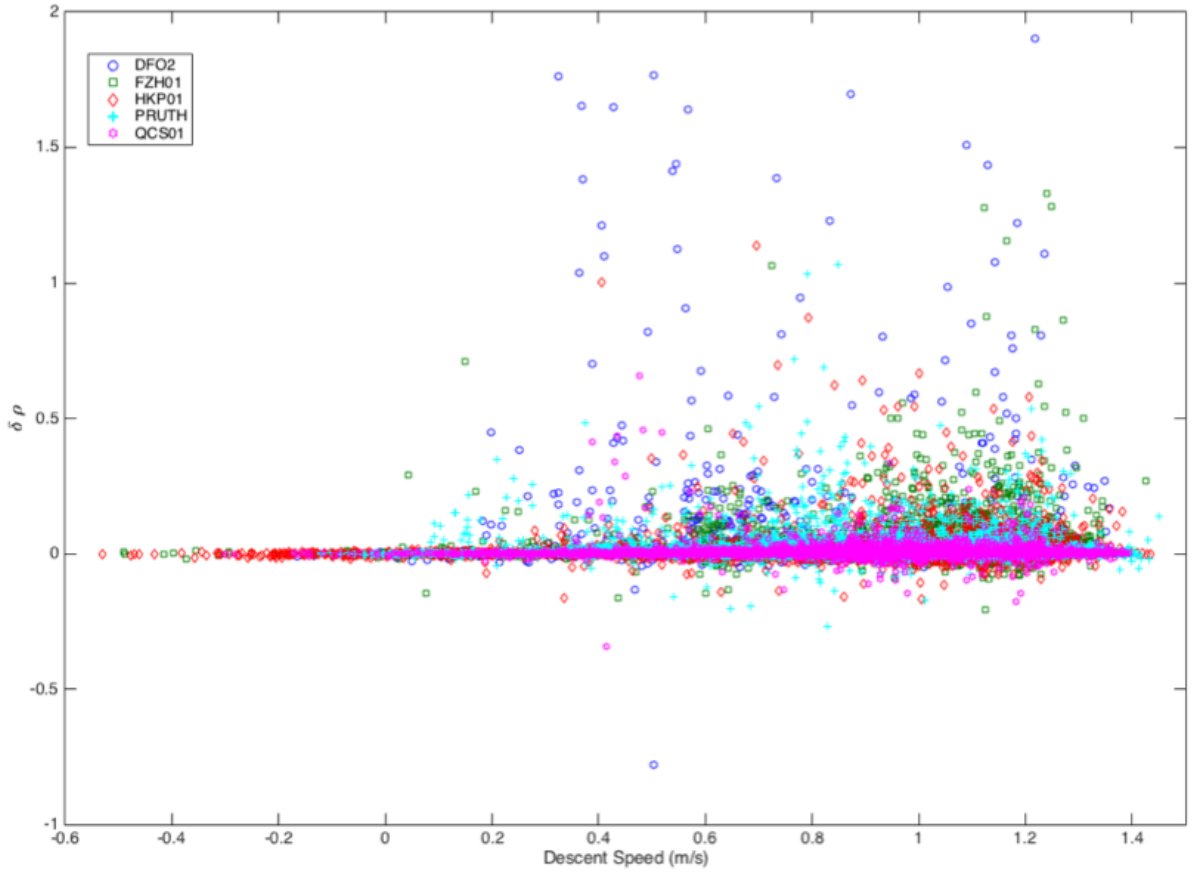

Figure 15: Scatter plot of the descent speed versus the first derivative of density for five different stations on the British Columbia central coast near Calvert Island. For each station, 1 year of data (which corresponds to 9 - 34 profiles) was examined. The stations sampled were DFO2, FZH01, HKP01, PRUTH, and QCSOQ (see www.hakai.org for a map).

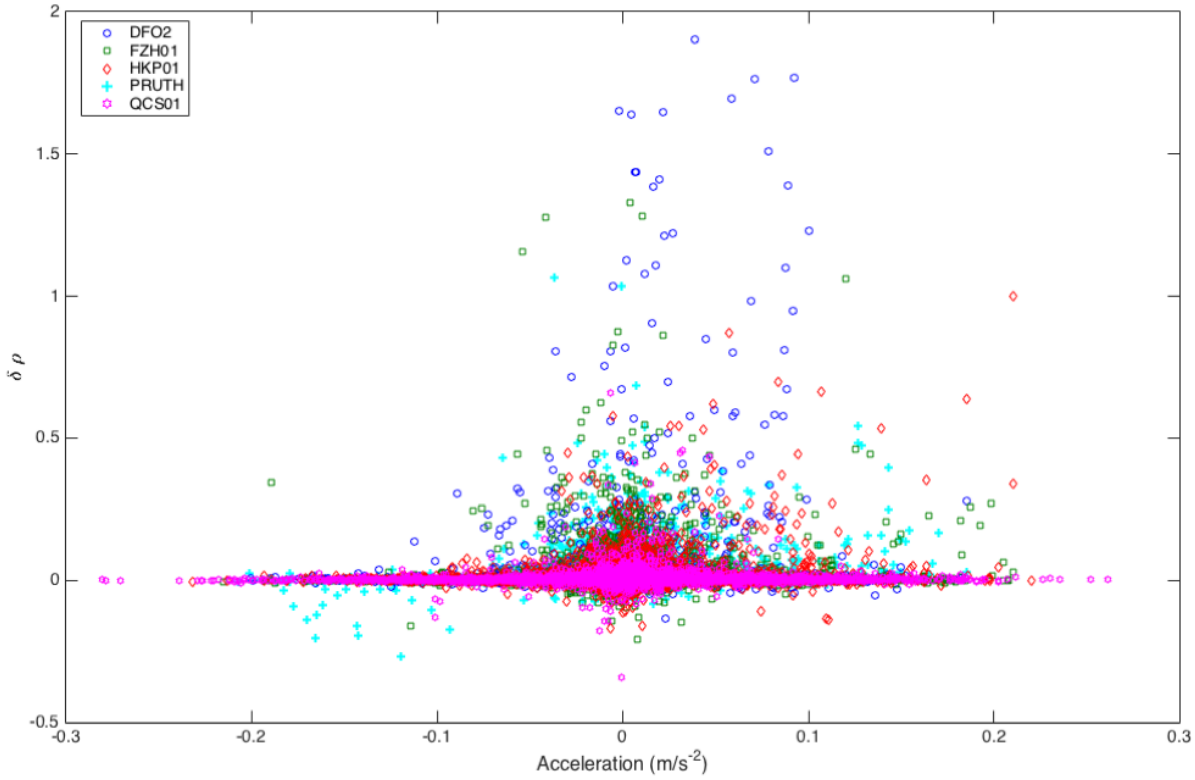

Figure 16: Scatter plot of the first derivative of descent speed versus the first derivative of density ($\delta\rho$) at five stations along the British Columbia central coast. Negative values of acceleration indicate deceleration and positive values indicate acceleration.

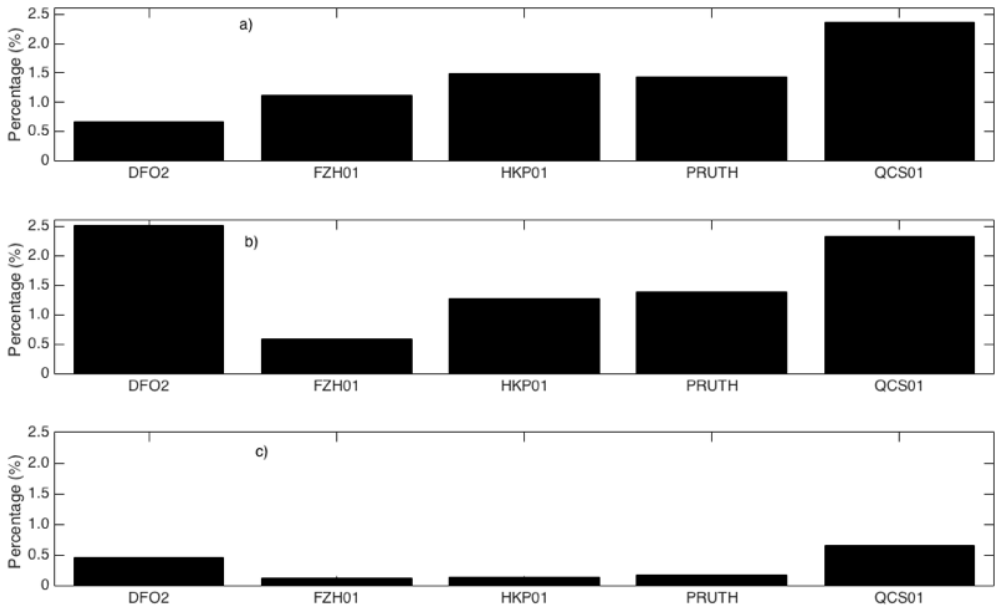

Figure 17: The percentage of raw data where a) the first derivative of density was less than -0.01 kg/m^3, which suggests a density inversion, b) the first derivative of descent speed was negative (suggesting deceleration) and descent speed was slower than 0.4 m/s, and c) the first derivative of descent speed was less than -0.1 m/s^2 and drop speed was slower than 0.4 m/s. Here only raw data that were taken during the downcast after the surface soak were included.

References

Henry C. Bittig, Bjorn Fiedler, Roland Scholz, Gerd Krahmann, and Arne Kortzinger. Time response of oxygen optodes on profiling platforms and its dependence on flow speed and temperature. *Limnology and Oceanography: Methods*, 12:617–636, 2014. doi: 10.4319/lom.2014.12.617.

Rolf G. Lueck. Thermal inertia of conductivity cells: Theory. *Journal of Atmospheric and Oceanic Technology*, 7(5):741–755, 1990. doi: 10.1175/1520-0426(1990)007⟨0741:TIOCCT⟩2.0.CO;2. URL http://dx.doi.org/10.1175/1520-0426(1990)007<0741:TIOCCT>2.0.CO;2.

Daisuke Sasano, Masao Ishii, Takashi Midorikawa, Toshiya Nakano, Takayuki Toxkieda, and Hiroshi Uchida. Testing a new quick response oxygen sensor,"RINKO". *Papers in Meteorology and Geophysics*, 62:63–73, October 2011. doi: 10.2467/mripapers.62.63.

Raymond W. Schmitt, Robert C. Millar, John M. Toole, and W. David Wellwood. A double-diffusive interface tank for dynamic-response studies. *Journal of Marine Research*, 63:263–289, 2005.

I. Shkvorets and F. Johnson. Advantages in performance of the RBR conductivity channel with Delrin^{TM}/ceramic inductive cell. In *OCEANS 2010 MTS/IEEE SEATTLE*, pages 1–8, Sept 2010. doi: 10.1109/OCEANS.2010.5664276.

A Example processing scheme

A typical implementation of the recommended processing steps would be the following. The starting point is a single raw RBR profile. The code below is written Matlab, using functions from the RBRproc Matlab toolbox and the TEOS-10 Gibbs Seawater toolbox.

```
%% correct for zero-order hold scans (if necessary)
profile = correctHoldRBR(profile,'interp');

%% remove atmospheric pressure from total pressure
profile = rmPatmRBR(profile);

%% despike Chlorophyll-a and turbidity
profile = despikeRBR(profile,{'Turbidity','Chlorophyll'},'median',3,'NaN');

%% low pass filter T/C
profile = filterRBR(profile,{'Conductivity','Temperature'},3);

%% delay conductivity by 0.3 seconds (2 scans at 6 Hz)
profile = alignRBR(profile,'Conductivity',-2/6); % negative means delay

%% advance Rinko oxygen by 3 seconds
profile = alignRBR(profile,'DissolvedO2',3);

%% advance Chl, Turb, and PAR by 0.3 seconds
profile = alignRBR(profile,{'Chlorophyll','Turbidity','PAR'},0.3);

%% filter for descent rate and acceleration, replace suspect data with NaN
profile = loopRBR(profile,'NaN');

%% derive some basic quantities
ind = ~strcmp(profile.units,'PSU');
profile.units = profile.units(ind);
profile = rmfield(profile,'Salinity'); % remove RBR's calculation

profile.PracticalSalinity = gsw_SP_from_C(profile.Conductivity,...
                                          profile.Temperature,...
                                          profile.Pressure);
profile.units(end+1) = {'PSU'};

%% calculate oxygen concentration from percent saturation

filtered = profile; % clone the profile

% smooth SP, T, O2 to match their time constants
```

```
fltr = blackman(17)/sum(blackman(17)); % approx 3 sec at 6 Hz
filtered = filterRBR(filtered,{'PracticalSalinity','Temperature','DissolvedO2'},fltr);

% calculate a bunch of variables needed for saturation value
filtered.AbsoluteSalinity = gsw_SA_from_SP(filtered.PracticalSalinity,...
                                           filtered.Pressure,...
                                           longitude,latitude);
filtered.units(end+1) = {'g/kg'};

filtered.PotTemperature = gsw_pt0_from_t(filtered.AbsoluteSalinity,...
                                         filtered.Temperature,...
                                         filtered.Pressure);
filtered.units(end+1) = {'deg C'};

filtered.ConTemperature = gsw_CT_from_t(filtered.AbsoluteSalinity,...
                                        filtered.Temperature,...
                                        filtered.Pressure);
filtered.units(end+1) = {'deg C'};

filtered.PotentialDensity = gsw_sigma0(filtered.AbsoluteSalinity, ...
                                       filtered.ConTemperature);
filtered.units(end+1) = {'kg/m^3'};

% calculate saturation value of water with Garcia & Gordon (1990)
filtered.DOsat = gsw_O2sol_SP_pt(filtered.PracticalSalinity,filtered.PotTemperature);
filtered.units(end+1) = {'umol/kg'};

filtered.DOConcentration = 0.01*filtered.DissolvedO2.*filtered.DOsat;
filtered.units(end+1) = {'umol/kg'};

filtered.DOConcentration2 = filtered.DOConcentration.*(filtered.PotentialDensity+1000)
filtered.units(end+1) = {'ml/l'};

% take the relevant parameters from 'filtered' and put them back into 'profile'
profile.DOsat = filtered.DOsat;
profile.units(end+1) = {'umol/kg'};

profile.DOConcentration = filtered.DOConcentration;
profile.units(end+1) = {'umol/kg'};

%% trim the soak and deck data, select only downcast
profile = trimRBR(profile);

%% bin by depth to 1 meter intervals
bin = binRBR(profile,'depth',1);
```